

Computer Simulations of Polyisoprene Local Dynamics in Vacuum, Solution, and the Melt: Are Conformational Transitions Always Important?

Neil E. Moe and M. D. Ediger*

Department of Chemistry, University of Wisconsin, Madison, Wisconsin 53706

Received February 8, 1996; Revised Manuscript Received April 30, 1996[®]

ABSTRACT: Molecular dynamics computer simulations have been performed on an isolated polyisoprene chain at 298 K. Simulations of polyisoprene in the melt (413 K) and in solution (298 K) have been previously reported. The local dynamics of polyisoprene chains in these three environments are compared. While conformational transition rates are similar in each environment, orientation correlation times for C–H bond vectors vary by a factor of 20. These simulation results are inconsistent with the common assumption that conformational transitions are largely responsible for the decay of the orientation correlation functions for C–H vectors. Substantial C–H vector relaxation results from coupled small amplitude motions of groups of adjacent torsions which do not involve conformational transitions. This mechanism plays a major role in C–H vector reorientation in the dilute solution simulations and also has a substantial influence in the melt simulations.

I. Introduction

Local polymer dynamics play an important role in determining bulk properties of polymers such as the temperature dependence of the viscosity and the glass transition temperature T_g . Experimental evidence for this includes NMR^{1,2} and dielectric relaxation^{3,4} data which indicate that local dynamics have a temperature dependence quite similar to that of the viscosity. These experiments are sensitive to the reorientation of C–H bond vectors in the case of the NMR and dipole moment vectors in the case of dielectric relaxation.

Many theories of local polymer dynamics have been developed over the last 30 years.^{5–15} Each of these recognizes that torsional degrees of freedom in the chain backbone are responsible for local chain motion. In these theories, transitions from one conformational state to another are generally assumed to be either the only or the most important type of torsional motion. This assumption is also often used in interpreting experimental results. For example, the experimental activation energy for C–H vector or dipole reorientation in polymer solutions has been used to calculate the potential energy barrier between conformational states.^{16–19} These potential barriers are presumed to be one feature which determines T_g for the neat polymer. As another example, data on C–H vector reorientation in polymer melts has been used to infer the nature of conformational transitions associated with the glass transition relaxation.^{20–22} Thus, the assumption that conformational transitions and C–H vector reorientation are tightly coupled permeates the theoretical and experimental literature.

Surprisingly, there is little evidence of a direct connection between conformational transitions and experimental observables such as C–H vector autocorrelation functions. Most experiments cannot measure conformational transition rates in polymers. The most relevant results come from pioneering two-dimensional NMR experiments by Spiess and co-workers.²³ These results indicate that the average time for conformational transitions is similar to the C–H vector correlation time for temperatures near T_g in atactic polypropylene melts.

For $T \gg T_g$, simulations can offer insight into the relationship between C–H vector reorientation and conformational transitions since both can easily be calculated from the same trajectory. However, most simulations to date have not illuminated this issue since calculations of experimental vector autocorrelation functions are usually omitted. Where both quantities have been calculated, it has been found that conformational transition rates and bond vector correlation times have somewhat different temperature dependences.^{24,25}

Two recent theories of local polymer dynamics by Perico¹⁴ and Moro¹⁵ do not *a priori* assign conformational transitions the dominant role in local polymer dynamics. Moro considers both conformational transitions and “coupled librations” to be important in determining local polymer dynamics. Coupled librations are cooperative, small amplitude motions of groups of adjacent torsions which do not involve conformational transitions. In other related work, Mansfield²⁶ showed that the end-to-end distance of a polymer chain can undergo large changes without any conformational transitions.

Here we present a comparison of the local dynamics of polyisoprene in the melt,²⁷ in dilute toluene solution,²⁸ and as an isolated chain in vacuum, based on molecular dynamics simulations. While the conformational transition rates are similar in each environment, the orientation correlation times for C–H bond vectors vary by a factor of 20. If conformational transitions were solely responsible for C–H vector reorientation in polyisoprene, one would expect that the correlation times should be roughly proportional to the time between conformational transitions. Our puzzling results can have two possible explanations. Either conformational transitions have much different characters in the three environments, or some other mechanism in addition to conformational transitions is significantly influencing the C–H vector correlation times. Our analyses of conformational transitions indicate that they are quite similar in the three environments. Thus, the second option appears the more likely explanation. We have found that coupled librations influence C–H vector correlation functions to a considerable extent at all times in all environments. This mechanism largely

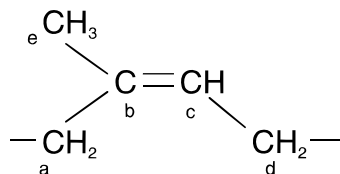
accounts for C–H vector reorientation in the isolated chain (conformational transitions play little role) and plays a major role for polyisoprene in dilute toluene solution. Only in the melt do conformational transitions have a major (but not overwhelming) effect on C–H vector reorientation.

The organization of this paper is as follows. In section II we present details of the isolated chain simulation and briefly describe all three simulations. Section III compares the local dynamics of polyisoprene in the melt, solution, and vacuum. Section IV considers the role which conformational transitions play in each of the three environments and presents evidence for a mechanism involving coupled librations. The final section considers the reliability and generality of these results.

II. Simulation Descriptions

We have previously reported molecular dynamics simulations on polyisoprene chains in the melt²⁷ and in an 11% solution with toluene.²⁸ Here we describe the simulation of an isolated polyisoprene chain in a vacuum in the context of this previous work. Our purpose in performing a simulation of an isolated chain was not to realistically model the dynamics of a chain in a vacuum. Such a chain would almost certainly be a collapsed globule. Rather, we wished to simulate an isolated chain with roughly the same dimensions as a melt or solution chain, but without any other molecules present to hinder its motion. Thus our vacuum simulation approximates a “zero-viscosity solution”. This effect was achieved by truncating the nonbonded interactions at a small distance.

The polyisoprene chains in all three simulations were 100% *cis* and had all head-to-tail linkages; the structure is



The vacuum and solution simulations used chains with 35 repeat units, while the melt simulations used chains with 100 repeat units.

The procedures used for the melt²⁷ and solution²⁸ simulations were also used for the isolated chain simulations except as noted below. Biosym's CFF91 force field²⁹ was used in each case and the simulations were performed using *InsightII*, *Amorphous Cell*, and *Discover*.³⁰ The temperature was held constant at 413 K in the melt simulations, and at 298 K for the solution and vacuum simulations. The pressure was held constant at 1 atm in the melt and solution simulations, and periodic boundary conditions were used. Periodic boundary conditions were not used in the vacuum simulations. The nonbonded potential was truncated after 8 Å in the melt and solution; a 6 Å cutoff was employed in the vacuum to prevent the chain from collapsing into a globule. A 1 fs time step was used for all the simulations.

The starting configuration for the isolated chain simulation utilized random torsional angles. After 100 steps of energy minimization, the system was equilibrated at 298 K for 250 ps. After this, coordinates were saved every 0.1 ps for 2 ns. The average end-to-end distance $\langle r^2 \rangle^{0.5}$ and radius of gyration $\langle r_g^2 \rangle^{0.5}$ were 43 and

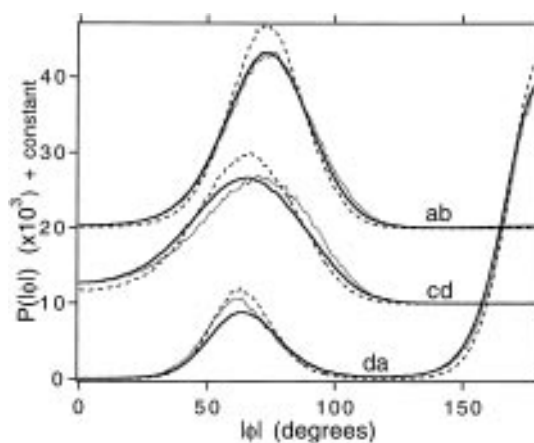


Figure 1. Symmetrized population distributions for torsions in the melt at 413 K (—), solution at 298 K (···), and vacuum at 298 K (---). For clarity, cd torsions have been displaced by +10 and ab torsions by +20.

18 Å, respectively. These values are in good agreement with the expected values for a 35-mer in solution and similar to those obtained from our simulations of a 35-mer in toluene.²⁸ These results, and the observation that significant fluctuations occur in both of these quantities, establish that the isolated chain behaved as a typical random coil.

In order to minimize end effects, the five repeat units at each chain end are excluded from all calculations described in sections III and IV.

Torsion Populations. The polyisoprene backbone has three different types of carbon–carbon single bonds per repeat unit. We refer to these three torsions as ab, cd, and da (see structure above). Figure 1 shows symmetrized population distributions for these three torsions from the melt, solution, and vacuum simulations. The effective potentials (a potential of mean force) for each of the torsions can be inferred from the figure using the relationship $\ln[P(\phi)] = -E(\phi)/RT$. The effective potential for torsion da has three wells while torsions ab and cd are two-fold; torsion cd is more “loose” (i.e., lower barrier) than torsion ab. Definitions of ϕ for the various torsions are as follows: $\phi = 0$ for torsions ab and cd was defined to place all the carbon atoms in the same plane, as in the structure above; for torsion da, the *trans* state was defined to be $\phi = 180^\circ$.

Clearly, the population distributions are very similar for polyisoprene chains in each of the three environments. The vacuum is slightly different from the other two environments in that the effective wells are somewhat deeper and narrower.

III. Comparison of Local Dynamics in the Melt, Solution, and Vacuum

This section compares the local dynamics of polyisoprene from simulations in three different environments. The dynamics considered fall into three categories: vector reorientation, carbon atom displacement, and torsional motion. Some calculations on the isolated chain are included to preserve continuity between this paper and the previous two. A striking observation is that C–H vectors lose their orientation on very different time scales in the three simulations, while differences in conformational transition rates and torsional motion are small. Section IV discusses this observation.

A. Vector Reorientation. C–H Vector Autocorrelation Functions. Experiments such as dielectric

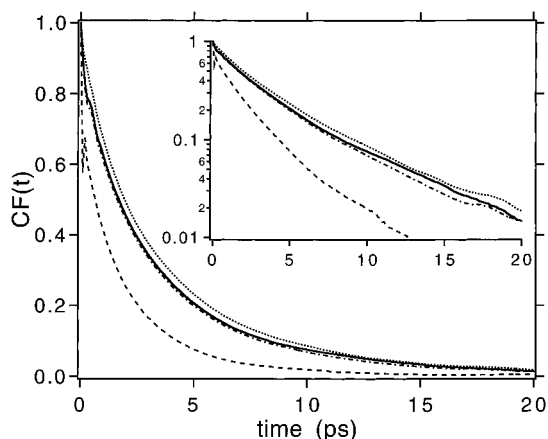


Figure 2. P_2 orientation autocorrelation functions for polyisoprene C-H bond vectors a (—), c(···), d(---), and e (- - -) from the vacuum simulation. The inset shows a semilogarithmic plot of the same curves, indicating that the correlation functions are nonexponential.

relaxation and NMR measure the reorientation of some vector fixed in the local molecular frame. ^{13}C and ^2H NMR relaxation experiments can measure the reorientation times of C-H (or C-D) bond vectors which depend upon the decay of the P_2 orientation autocorrelation function:

$$CF(t) = \langle P_2(\hat{x}(0) \cdot \hat{x}(t)) \rangle = \langle 3 \cos^2 \Theta(t) - 1 \rangle / 2 \quad (1)$$

Here P_2 is the second Legendre polynomial, $\hat{x}(t)$ is a unit vector in the direction of a particular C-H vector at time t , and $\Theta(t)$ describes the orientation of the vector at time t relative to its orientation at time 0. The orientation correlation time τ_c is the time integral of the correlation function:

$$\tau_c = \int_0^\infty CF(t) dt \quad (2)$$

Rapidly decaying correlation functions result in small τ_c 's and imply fast dynamics. Both the autocorrelation functions and their integrals are readily obtained from the simulation trajectories.

Figure 2 shows the P_2 autocorrelation functions for C-H vectors a, c, d, and e calculated from the vacuum simulation. The three backbone C-H vectors (a, c, d) reorient on roughly the same time scale, while the methyl C-H vector reorients more rapidly due to nearly free rotation about the C-C bond. The order of the correlation function decays in vacuum is identical to those in the melt and solution (e is faster than d is faster than a is faster than c). The inset in Figure 2 shows a semilog plot of the same functions. The curves are clearly nonexponential.

Figure 3 shows the correlation function decays for C-H vector c in the melt, solution, and vacuum. Not surprisingly, C-H vectors reorient faster when the medium is less restrictive.³¹ The correlation times τ_c associated with these correlation functions are compiled in Table 1 for the melt, solution, and vacuum. τ_c values for the vacuum simulation were obtained by numerical integration out to 50 ps.

Motion of Vectors Parallel and Perpendicular to the Chain Backbone. Following Takeuchi and Roe,³² we have analyzed the anisotropy of local dynamics by calculating correlation functions for vectors parallel and perpendicular to the chain backbone. $1/e$ times for the P_1 and P_2 autocorrelation functions are shown

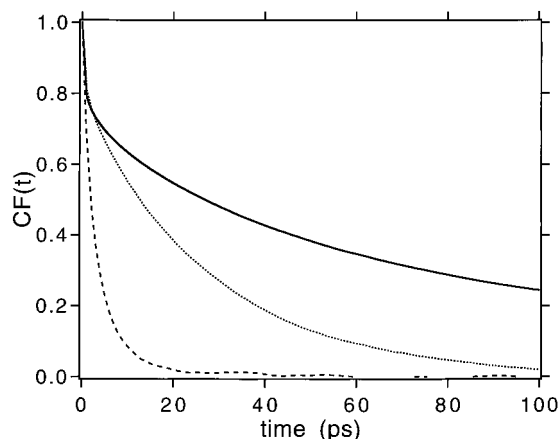


Figure 3. P_2 orientation autocorrelation functions for C-H vector c in the three environments. The labeling scheme is the same as in Figure 1. C-H vectors reorient very differently in the melt, solution, and vacuum. As discussed below, conformational transition rates are similar in the three environments.

Table 1. C-H Vector Correlation Times τ_c (ps)

C-H vector	melt ^a (413 K)	solution ^b (298 K)	vacuum (298 K)
a	65	20.3	3.4
b	89	22.2	3.8
c	55	18.6	3.2
d	9.4	3.7	1.5

^a Reference 27. These times include the estimated contribution of the long tail of the correlation function. ^b Reference 28.

Table 2. $1/e$ Relaxation Times for Vectors Parallel and Perpendicular to the Chain Axis (ps)

	melt ^a (413 K)	solution (298 K)	vacuum (298 K)
$P_1(\parallel)$	387	67	10.8
$P_2(\parallel)$	63	25	3.6
$P_1(\perp)$	107	54	8.5
$P_2(\perp)$	38	19	2.8
$P_1(\parallel)/P_1(\perp)$	3.6	1.2	1.3
$P_2(\parallel)/P_2(\perp)$	1.7	1.3	1.3

^a Reference 27.

in Table 2; the details of the calculation are given in ref 27. The P_1 function is $\langle \cos \Theta(t) \rangle$, and P_2 is given by eq 1. For either P_1 or P_2 , a ratio of parallel and perpendicular $1/e$ times of about unity indicates essentially isotropic local dynamics. Table 2 indicates that motion is somewhat less isotropic in the melt than in solution or vacuum. The more constricting melt environment preferentially inhibits reorientation of the chain backbone. In all environments, the anisotropy of polyisoprene local dynamics is much less pronounced than in simulations of polyethylene melts by Takeuchi and Roe.^{32,33}

B. Carbon Atom Displacement. Another indication of the local mobility of polyisoprene chain segments in the three different environments is the average displacement of chain atoms in a given amount of time. Figure 4 shows the mean displacement of carbon atoms versus time in the melt, solution, and vacuum. In spite of the higher temperature of the melt simulation (413 K vs 298 K), after the first few picoseconds carbon atoms in the melt are more constrained than in the other two environments.

C. Torsional Motion. Time Evolution of Torsional Coordinates. Figure 5 shows the probability of observing an angular change $|\Delta\phi|$ during various time intervals for the three-fold torsion ϕ for polyisoprene chains in the three environments. Many torsions have

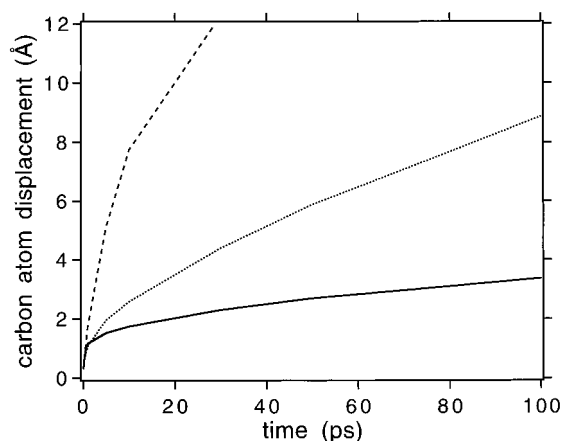


Figure 4. Mean distance traveled by carbon atoms in polyisoprene at various times. The labeling scheme is the same as in Figure 1. Carbon atom mobility is very different in the three environments, while conformational transition rates are similar.

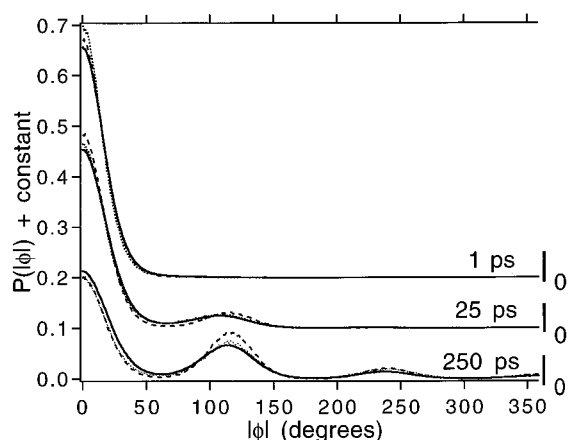


Figure 5. Probability P of an angular change $|\Delta\phi|$ for torsion da in various time intervals. The three different curves correspond to the three environments; the labeling scheme is the same as in Figure 1. Librational motions in the bottom of potential wells equilibrate in less than 1 ps. Conformational transitions occur at much longer times. There are no major differences between the three environments even though C–H vectors reorient on much different time scales.

already adjusted by 10–30° within the first picosecond. The width at half-height of this feature of the distribution changes little as time evolves. At much longer times, population is lost from this part of the distribution and new peaks centered at 120 and 240° grow in, indicating transitions to other conformational states. Thus fast motions within potential wells cause the equilibrium distribution of angles to be reached within a potential well before a significant number of conformational transitions occur. At all times, the angular evolution of torsional coordinates is very similar in the three different environments. In particular, this is the case for $t = 25$ ps, even though the C–H vector autocorrelation functions (Figure 3) and carbon atom displacements (Figure 4) show very different behaviors by this time.

Comparison of Transition Rates in the Melt, Solution, and Vacuum. In order to discuss conformational dynamics in polymers, one must choose a particular definition of a conformational transition. We define a conformational transition to occur when a torsion angle moves from the minimum of one potential well to the minimum of a neighboring well (see Figure 1). We use the *last* time the torsion crossed the barrier

Table 3. Conformational Transition Times (ps)

torsion	melt ^a (413 K)	solution ^b (298 K)	vacuum (298 K)
ab	97	238	210
cd	63	93	39
da	90	104	129
average	81	122	79

^a Reference 27. ^b Reference 28.

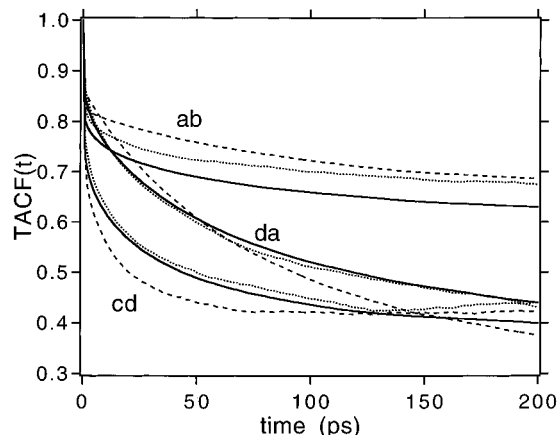


Figure 6. P_2 torsion autocorrelation functions for torsions ab, cd, and da in the melt (—), solution (···), and vacuum (---).

peak on the way to the second well bottom as the transition time τ_{trans} . There are other reasonable ways to define a conformational transition, but we do not believe that adoption of one of these would change our conclusions. We test this in one calculation below.

Polyisoprene has three different torsions per repeat unit, and the conformational transitions of each had distinct characteristics in our simulations. Table 3 contains transition times for the three torsions of polyisoprene in the three environments.³⁴ Although there are some noticeable differences between the different simulations (e.g., the relative importance of transitions at ab and cd torsions changes as the restrictiveness of the environment changes), the overall average time between transitions is very similar in the three environments. Different simulation temperatures (413 K for melt, 298 K for solution and vacuum) are partially responsible for the similar average transition times.

It is surprising that the average time between conformational transitions is similar in the melt, solution, and vacuum simulations given that C–H vector correlation times and carbon atom displacements are very different in these environments. The ratios of the average transition times and the average correlation times τ_c for backbone C–H vectors is about 1 in the melt, 6 in solution, and 23 in vacuum. This result questions the existence of a direct connection between conformational transitions and C–H vector reorientation.

Torsion Autocorrelation Functions. We have also calculated P_2 autocorrelation functions for the various torsions in the simulations:

$$TACF(t) = \langle 3 \cos^2(\Delta\phi(t)) - 1 \rangle / 2 \quad (3)$$

where $\Delta\phi(t)$ is $\phi(t) - \phi(0)$. Figure 6 shows these functions for the three torsions of polyisoprene in the three environments. Note that these functions do not decay to zero at infinite time, but rather reach a plateau near the values shown at $t = 200$ ps.

It can be seen that the decays are relatively unaffected by the environment of the chains. For the cd torsion, relaxation is somewhat faster in vacuum than

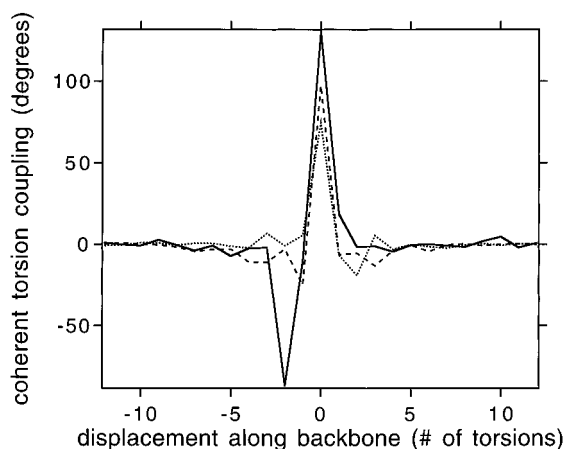


Figure 7. Change in neighboring torsion angles accompanying a conformational transition at position zero (eq 4, $\Delta t = 0.5$ ps) for polyisoprene in the vacuum. The change relative to the rotation sense of the transforming bond is shown for torsions ab (—), cd (···), and da (---). For example, for a transition at an ab torsion, position -1 is a da torsion, positions +1 and -2 are cd torsions, etc. Most torsion adjustments occur within one repeat unit of the transforming bond.

in the melt; for the ab torsion, relaxation is faster in the melt than in vacuum. Even these small differences are less apparent if one accounts for the non-zero values of the correlation functions at infinite time.³⁵

Coupling Analysis of Conformational Transitions. Conformational transitions in a polymer backbone are not completely isolated events. Other degrees of freedom play a major role in localizing and thereby facilitating conformational transitions. The degree to which conformational transitions are localized in polyisoprene can be illustrated using two calculations. Conceptually, we take snapshots of the atoms near a conformational transition just before and after the transition occurs (at time τ_{trans}). We can then ask how various degrees of freedom evolved in the time interval ($2\Delta t$) between the two snapshots. The first calculation examines how neighboring torsions change their orientation as a function of distance along the chain away from the triggering transition. A second calculation examines how C-H vectors along the backbone reorient in response to a conformational transition. This calculation was undertaken because we are specifically interested in how conformational transitions effect C-H vector motion. For both calculations, we average over all transitions of a given type (ab, cd, or da) which occur in each simulation.

The average angular displacement of a torsional coordinate ϕ in response to a triggering conformational transition is calculated as follows:

$$\langle A(\Delta\phi) | \phi(\tau_{\text{trans}} + \Delta t) - \phi(\tau_{\text{trans}} - \Delta t) \rangle \quad (4)$$

Here $A(\Delta\phi)$ is chosen to be ± 1 in order to isolate torsional motion in the same direction as the triggering transition. If a torsion rotates in the same direction as the triggering transition, it counts positively to the average. Position 0 on the abscissa is defined by the conformational transition and positive values represent neighboring torsions to the right along the chain. Note that the double bond (torsion bc) is not included in this analysis.

Figure 7 shows the results of using expression 4 to analyze the polyisoprene vacuum simulation. The maximum angular distortion is found at position 0 for each torsion type. On either side of position 0, the

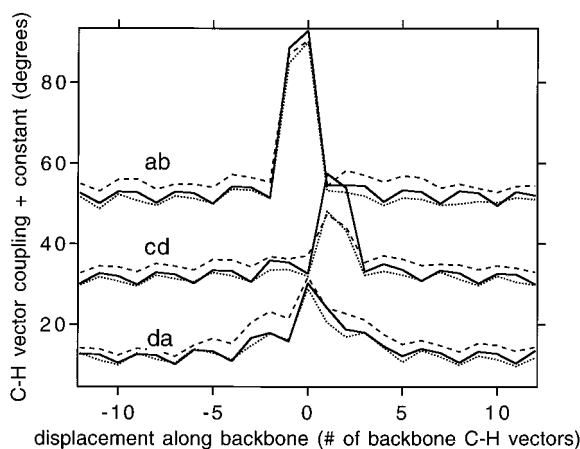


Figure 8. Change in orientation of C-H bond vectors near a conformational transition occurring between bond vectors 0 and 1 (eq 5, $\Delta t = 0.5$ ps). For example, for a transition at an ab torsion, position 0 is C-H vector a, position +1 is C-H vector c, positions +2 and -1 are C-H vector d, etc. Conformational transitions have similar effects on C-H vector reorientation in the three environments (labeled as in Figure 1) with most orientation changes occurring within one repeat unit of the transforming bond. For clarity, plots for cd transitions are displaced by $+20^\circ$ and those for ab transitions by $+40^\circ$.

baseline goes to zero since torsions far away from the triggering transition are equally likely to rotate in either sense. Figure 7 indicates that the region of cooperative motion involving neighboring torsions is largely limited to three to four torsions in the vacuum, or about one repeat unit. Similar results were presented for melt and solution simulations in references 27 and 28. The major difference between the vacuum results and the others is that the magnitude of the peak at +2 for torsion cd is smaller in the vacuum. This indicates that conformational transitions at a cd torsion require little cooperation from neighboring ab torsions. This relative freedom is reflected in the large conformational transition rate of the cd torsion in vacuum (see Table 3).

The second coupling analysis considers how conformational transitions are correlated with the reorientation of nearby C-H vectors. Mathematically, the following expression is evaluated:

$$\langle \arccos(\hat{x}(\tau_{\text{trans}} + \Delta t) \cdot \hat{x}(\tau_{\text{trans}} - \Delta t)) \rangle \quad (5)$$

Figure 8 shows the average change in the orientation of C-H vectors during the time window $\tau_{\text{trans}} \pm \Delta t$ ($\Delta t = 0.5$ ps) as a function of position on the chain backbone relative to the triggering conformational transition. Vectors near a conformational transition reorient the most in $2\Delta t$ while those farther than one repeat unit away appear to be unaffected by the triggering transition regardless of the environment. The baseline represents motion uncoupled to the triggering transition. This motion is greatest in the isolated chain, consistent with the correlation functions plotted in Figure 3.

IV. Discussion

The results presented in the previous section are surprising. C-H vector correlation functions and carbon atom displacements indicate that the local dynamics of polyisoprene chains are very different in the melt, solution, and vacuum. In contrast, conformational transition rates are very similar in the three different environments. Quantitatively, the ratio of the average time between transitions and the average τ_c for back-

bone C–H vectors is 1 in the melt, 6 in solution, and 23 in vacuum. These results question the standard assumption that conformational transitions are tightly coupled to C–H vector reorientation.

In this section we present an explanation for these results. Significant C–H vector reorientation for polyisoprene in solution and in a vacuum occurs without conformational transitions. A mechanism of “coupled librations” appears to play a very significant role in this process. These coupled librations also are important for C–H vector reorientation in the melt. The generality of these results and their implications are discussed in section V.

Polymer Motions Contributing to C–H Vector Reorientation. Many processes contribute in varying degrees to the reorientation of C–H bond vectors in polymers. High-frequency/low-amplitude motions like bond bending and stretching are not expected to play a major role. In principle, C–H vector reorientation could occur via rotation of the entire chain about its center of mass. For these polyisoprene simulations, we have verified that this is not the case since relaxation of the end-to-end vector occurs several orders of magnitude slower than the C–H vector correlation function decays. By eliminating the alternatives, we conclude that C–H vector reorientation in our simulations must occur primarily by changes in the torsional coordinates.

There are two well-recognized types of torsional motion known to play a role in C–H vector reorientation. On very short time scales (on the order of 1 ps), torsional degrees of freedom explore the bottom of a potential well. These librational motions are illustrated by the top set of curves in Figure 5. As shown in Figure 3, librations cause the C–H vector autocorrelation functions for polyisoprene to lose around 25% of their initial values in the first picosecond. On much longer time scales, large torsional displacements result from conformational transitions from one potential well to another (see lower curves in Figure 5). Usually, it is assumed that these motions are responsible for the slowly decaying portion (i.e., times longer than 1 ps) of the C–H vector correlation functions. Since the correlation time τ_c is the integral of the correlation function, this longer decay has the predominant influence on τ_c . If conformational transitions cause this decay, then τ_c should be primarily determined by the average time for conformational transitions.

Clearly, this view is not consistent with the simulation results for polyisoprene in different environments. How can conformational transition rates be similar and yet C–H vector correlation times be very different? There can be two possible answers to this question. Either conformational transitions in the three environments differ significantly in their effect on C–H vector motion, or some type of motion other than conformational transitions contributes significantly to the slow part of the correlation function decay.

Are Conformational Transitions Significantly Different in the Melt, Solution, and Vacuum? We believe that this option can be dismissed on the basis of the evidence presented in section III. One interpretation of the ratios of conformational transition times to correlation times could be that a conformational transition fully reorients C–H vectors within, for example, 1 repeat unit in the melt, 6 repeat units in solution, and 23 repeat units in vacuum. Figures 7 and 8 show that this is not the case. In particular, Figure 8 shows that conformational transitions influence C–H vector reori-

entation within about 1 repeat unit in each environment.

Another possible explanation would be that there are many more back-transitions in the melt than in solution or vacuum and that these pairs of transitions essentially cancel each other out. This would have an effect similar to lowering the transition rate. As noted in ref 27, more back-transitions are found in the melt than in solution. However, the torsion angle autocorrelation functions plotted in Figure 6 indicate that torsional space is explored similarly in the three environments. In addition, the torsion spreading plots in Figure 5 are quite similar at 25 ps, at which time the C–H vector autocorrelation functions in Figure 3 are very different for the three environments. These two results are not consistent with the explanation that back-transitions are responsible for the variation in the ratios of average transition times to C–H vector correlation times.

Vector Correlation Functions Calculated without Conformational Transitions. The most direct way to test the importance of conformational transitions would be to run a second set of simulations using modified torsion potentials which disallow conformational transitions. This could be accomplished by placing a “spike” on top of the potential energy barriers while being careful not to modify the wells. Rather than doing a simulation with altered potentials, we recalculated C–H vector correlation functions using only those parts of the trajectory which are unaffected by conformational transitions. We first locate conformational transitions and block off a region about each of them in space and time. Correlation functions are then calculated for those parts of the trajectory between the blocked off sections. Figure 8 shows that the effect of conformational transitions on C–H vector reorientation is mostly confined to a single repeat unit. We chose to block off 1, 3, or 5 repeat units in this calculation.³⁶ We used a time window of $\Delta t = \pm 0.5$ ps about each conformational transition. This choice was based on calculations like those shown in Figure 8 in which various values of Δt were tested.

Figure 9 displays correlation functions for C–H vector *c* based only on sections of the trajectory without conformational transitions. The dotted line shows the result when 1 repeat unit is excluded about each transition while the dashed line illustrates the result if 3 repeat units are excluded. The correlation functions calculated by excluding 5 repeat units about each transition (not shown) are very similar to the dashed lines. These modified correlation functions are compared to the correlation functions calculated from the full trajectories (full lines). If conformational transitions were completely responsible for the slow decay of the correlation function, the dashed and dotted lines would be flat after a fast decay to ~ 0.75 . Clearly other mechanisms are allowing the correlation functions to decay.

We can roughly estimate the role which conformational transitions play in the slow part of the C–H vector correlation function decay by comparing the solid and dashed lines in Figure 9. By using the times when the functions reach $1/e$, we can estimate that other mechanisms are three times more important than conformational transitions in vacuum. In solution, other mechanisms are equally important as conformational transitions. In the melt, conformational transitions are 2–3 times more important than other mechanisms. As the restrictiveness of the environment

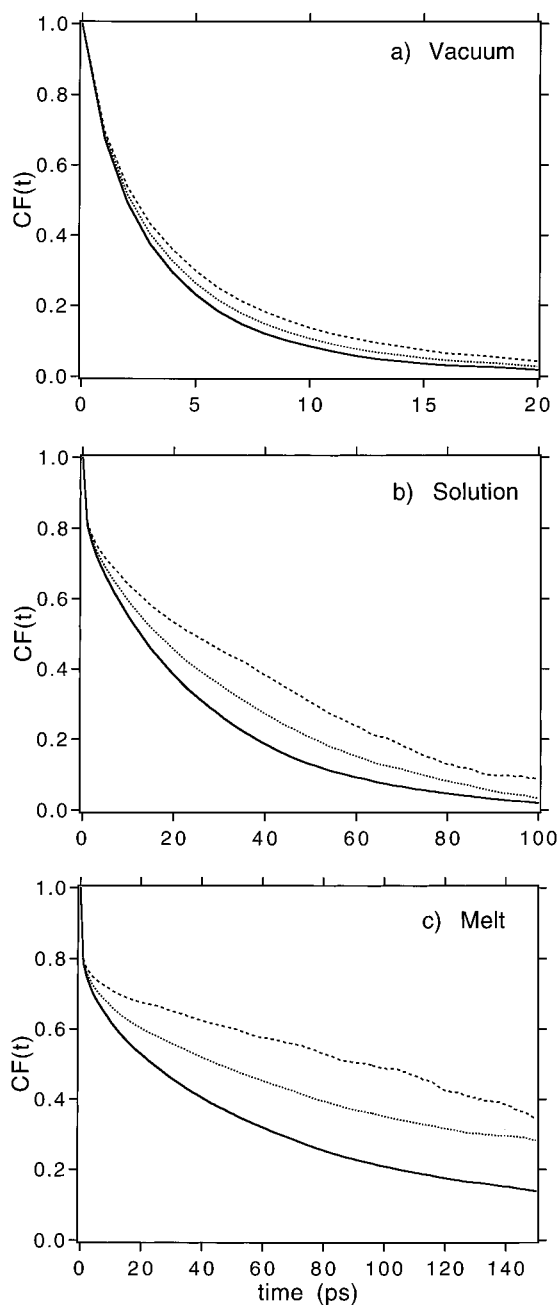


Figure 9. P_2 orientation autocorrelation functions for C-H bond vector c in vacuum (a), in solution (b), and in the melt (c). Included are the functions from the whole trajectory (—) and from subsets which exclude one (···) and three (---) repeat units about each conformational transition. C-H vectors can reorient substantially without conformational transitions in all three environments. Conformational transitions are responsible for the greatest fraction of C-H vector relaxation in the most restrictive environment.

increases, conformational transitions play a more important role in the C-H correlation function decay. Even in the melt, however, mechanisms other than conformational transitions appear to have a significant influence on the C-H vector correlation function decay.

Two additional calculations were performed to make certain that our modified correlation functions were not influenced by conformational transitions. We tested whether our definition of a conformational transition might be too restrictive by blocking off sections of the trajectory around every barrier crossing;³⁷ this did not have a major effect on the modified correlation functions. We also found that changing Δt from 0.5 and 5

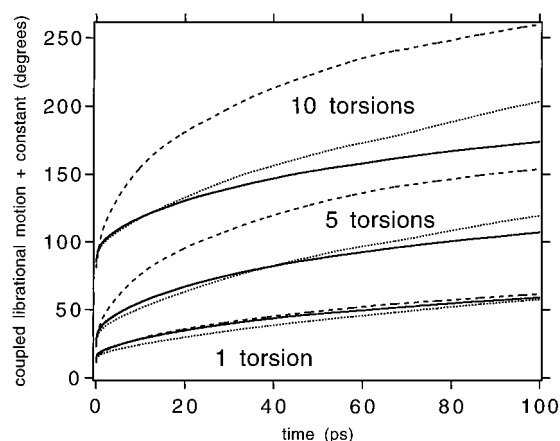


Figure 10. Collective motion of groups of 1, 5, and 10 torsions (eq 6, $n = 1, 5, 10$) in each environment (labeling scheme is the same as in Figure 1). The plot for 10 torsions is displaced by $+50^\circ$. Individual torsions show similar time evolution in each environment. Groups of 5 and 10 torsions show much more motion in the vacuum than in solution and in the melt. Differences in this coupled librational motion account qualitatively for the different C-H vector reorientation observed in the three environments.

ps yielded essentially identical results when one repeat unit was blocked off around a conformational transition.

How Can C-H Bond Vectors Reorient without Conformational Transitions? One way is for groups of torsions to move cooperatively so that small angular motions in many individual torsions add up to a large C-H vector reorientation. This effect can be illustrated by imagining a simplified polymer backbone consisting of 180° bond angles (i.e., a completely linear polymer) with C-H vectors perpendicular to the chain axis. If, for example, five sequential torsions all moved 10° clockwise, the C-H vectors along this portion of the chain would reorient an average of 30° . We believe that something like this type of motion plays a dominant role in C-H vector reorientation in vacuum and solution, and also plays a significant role in the melt. Following Moro,¹⁵ we refer to this mechanism as “coupled librations” in order to emphasize that individual torsional coordinates remain near the minimum in the potential well.

To test this picture of coupled librational motion, we have calculated the quantity

$$\left| \sum_{m=1}^n \Delta\phi_m(t) \right| \quad (6)$$

Here n is the number of contiguous torsions considered in the calculation, m is an index from 1 to n , and $\Delta\phi_m(t)$ is the angular change of torsion m in time t . All double bonds are excluded from the calculation. Figure 10 shows this quantity calculated for the melt, solution, and vacuum for $n = 1, 5$, and 10 . The curves for $n = 1$ are simply the absolute value of the average angular change of single torsions as a function of time; thus, the points in Figure 10 at $t = 1$ ps and 25 ps are first moments of distributions like those shown in Figure 5. Consistent with previous calculations, individual torsions evolve similarly in each of the three environments. However, the sets of curves for $n = 5$ and 10 are qualitatively different. Groups of torsions have much greater freedom in the vacuum than in the melt or solution. Groups of torsions in solution also have somewhat more freedom than in the melt.

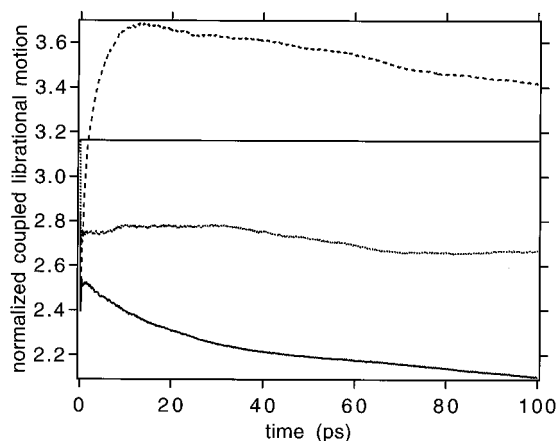


Figure 11. Collective motion of groups of 10 torsions normalized by the motion of single torsions. The labeling scheme for the three environments is the same as in Figure 1. The flat line at $10^{1/2}$ represents the random walk result for uncoupled torsions. The long-time results for melt and solution lie below this line, indicating that neighboring torsions tend to move in opposite senses, minimizing the net displacement of chain segments.

Figure 11 shows the curves for $n = 10$ normalized by the curves for $n = 1$ for each of the three environments. If the motion of each torsion were uncorrelated with its neighbors, the value of the average normalized displacement for 10 torsions would be $10^{1/2}$ (the random walk result). This is the line shown in Figure 11. It can be seen that the asymptotic result for the melt is well below the random walk limit, indicating that nearby torsions tend to move in opposite senses. This motion minimizes the net displacement of chain segments in a viscous medium. The result for solution is also below the random walk result but not to the same extent as the melt. In contrast, the curve for the isolated chain is above the random walk result. Thus, nearby torsions tend to move in the same sense. These trends imply that "coupled librations" are most important for polymers in less restrictive environments.

V. Concluding Remarks

We have presented a comparison of the local dynamics of polyisoprene chains in the melt, in dilute toluene solution, and in vacuum based on molecular dynamics computer simulations. While conformational transition rates are similar in each environment, C–H vectors reorient on very different time scales. Calculations of the C–H vector autocorrelation function using only those parts of the trajectory without conformational transitions clearly show that conformational transitions are not solely responsible for the major portion of the correlation function decays. Most C–H vector relaxation in vacuum and about half of the C–H vector relaxation in solution is achieved through cooperative motions of groups of torsions which do not involve conformational transitions. Even in the melt, these coupled librational motions play a significant role in C–H vector relaxation.

The theory by Moro¹⁵ for the dynamics of a rotor chain includes both conformational transitions and coupled librations. In this theory, librational motions contribute substantially to the rotor correlation function at all times, in qualitative agreement with our simulations. Extending this theory to incorporate actual chain geometries and potentials might result in a realistic description of the local polymer dynamics observed here.

The conclusion that C–H vector reorientation is not necessarily determined by conformational transition rates contradicts the prevailing view in the field of local polymer dynamics. *Do these simulations reflect reality?* We have previously shown that the solution and melt simulations are in reasonable agreement with NMR measurements which are sensitive to local polymer dynamics.^{27,28} Clearly, the isolated chain simulations are only suggestive. We anticipate that if a more realistic simulation of polyisoprene in solution or the melt is performed, coupled librations will be found to play a significant role in the orientational relaxation of C–H vectors. Simulations with a different force field could provide a valuable check.

What are the potential implications for the interpretation of experimental work on polymer solutions? Experiments on local dynamics in solution are often interpreted by assuming that the temperature dependence of C–H vector reorientation is directly related to the height of a potential barrier between conformational states. Since our simulations indicate that a mechanism other than conformational transitions plays a major role in C–H vector reorientation, this assumption may be in error and hence the calculated barrier heights may be incorrect. Simulations at various temperatures would be required to directly test this assumption.

What are the potential implications for the interpretation of experimental work on polymer melts? While it is well documented that C–H vector reorientation is directly related to the glass transition in bulk polymers, the glass transition is usually considered to be more fundamentally connected with the rate of conformational transitions. Significant differences in the temperature dependences for transition rates and C–H vector correlation times would make this interpretation suspect. These simulations raise this possibility since a mechanism other than conformational transitions is observed to play a role in C–H vector reorientation.

NMR experiments by Spiess and co-workers indicate that C–H vector motions and conformational transition rates have similar temperature dependences in atactic polypropylene near T_g .²³ Whether this is true for all polymers and also for temperatures far above T_g remains an open question. The polymer simulated here, polyisoprene, has relatively broad wells in the vicinity of several potential minima. These should increase the importance of coupled librations. In polymers with narrower wells, such as polypropylene, conformational transitions and C–H vector reorientation may be more tightly coupled.

One aspect of the NMR experiments²³ suggests that coupled librations might also play a role in polypropylene melts. These experiments found that C–H vector motion did not occur by large angle jumps such as those described by motion on a diamond lattice. Rather, C–H vector motion was "consistent with a sequence of small-angle and large-angle reorientations resulting from conformation transitions coupled to relaxation of longer chain units". It is possible that coupled librations might be responsible for the small-angle reorientations seen in the experiment.

In summary, the simulation results presented here certainly do not settle any issues regarding the connection between conformational transitions and C–H vector reorientation. These results indicate that an important assumption in the field of local dynamics *may* be incorrect in some cases. Further experimental and computational work is certainly in order. We hope that investigators running long simulations of polymer melts

or solutions might consider addressing these issues. A direct comparison of the temperature dependences of conformational transition times and C–H vector correlation times would be particularly useful.

Acknowledgment. This work was supported by the National Science Foundation (DMR-9424472). The computers used in this work were purchased through a grant from the NSF Chemistry Division (CHE-9007850). We thank Prof. Michael Fuson for helpful conversations.

References and Notes

- (1) Pschorn, U.; Rössler, E.; Sillescu, H.; Kaufmann, S.; Shaefer, D.; Spiess, H. W. *Macromolecules* **1991**, *24*, 398.
- (2) Schaefer, D.; Spiess, H. W.; Suter, U. W.; Fleming, W. W. *Macromolecules* **1990**, *23*, 3431.
- (3) Ferry, J. D.; Fitzgerald, E. R. *J. Colloid Sci.* **1953**, *8*, 224.
- (4) McCrum, N. G.; Read, B. E.; Williams, G. *Anelastic and Dielectric Effects in Polymer Solids*; Wiley: London, 1967.
- (5) Jones, A.; Stockmayer, W. *J. Polym. Sci., Polym. Phys. Ed.* **1977**, *15*, 847.
- (6) Bendler, J.; Yaris, R. *Macromolecules* **1978**, *11*, 650.
- (7) Gronski, W.; *Makromol. Chem.* **1977**, *178*, 2949.
- (8) McInnes, D.; North, A. *Polymer* **1977**, *18*, 505.
- (9) Anderson, J. *J. Chem. Phys.* **1970**, *52*, 2821.
- (10) Valeur, B.; Jarry, J.; Geny, F.; Monnerie, L. *J. Polym. Sci., Polym. Phys. Ed.* **1975**, *13*, 667.
- (11) Skolnick, J.; Yaris, R. *Macromolecules* **1983**, *16*, 266.
- (12) Helfand, E. *J. Polym. Sci., Polym. Symp.* **1985**, *73*, 39.
- (13) Hall, C. K.; Helfand, E. *J. Chem. Phys.* **1982**, *77*, 3275. Cook, R.; Helfand, E. *J. Chem. Phys.* **1985**, *82*, 1599. Skolnick, J.; Helfand, E. *J. Chem. Phys.* **1980**, *72*, 5489.
- (14) Perico, A. *Acc. Chem. Res.* **1989**, *22*, 336.
- (15) Moro, G. *J. Chem. Phys.* **1992**, *97*, 5749.
- (16) Mashimo, S.; Chiba, A. *Polym. J.* **1973**, *5*, 41.
- (17) Gronski, W.; Schafer, T.; Peter, R. *Polym. Bull.* **1979**, *1*, 319.
- (18) Radiotis, T.; Brown, G. R.; Dias, P. *Macromolecules* **1993**, *26*, 1445.
- (19) Zhu, W.; Gisser, D.; Ediger, M. D. *J. Polym. Sci., Part B: Polym. Phys.* **1994**, *32*, 2251.
- (20) Dejean de la Batie, R.; Lauprêtre, F.; Monnerie, L. *Macromolecules* **1989**, *22*, 122.
- (21) Denault, J.; Prud'homme, J. *Macromolecules* **1989**, *22*, 1307.
- (22) Bandis, A.; Inglefield, P. T.; Jones, A. A.; Wen, W.-Y. *J. Polym. Sci., Polym. Phys. Ed.* **1995**, *33*, 1515.
- (23) Zemke, K.; Chmelka, B. F.; Schmidt-Rohr, K.; Spiess, H. W. *Macromolecules* **1991**, *24*, 6874. Schaefer, D.; Spiess, H. W. *J. Chem. Phys.* **1992**, *97*, 7944.
- (24) Adolf, D.; Ediger, M. D. *Macromolecules* **1991**, *24*, 5834.
- (25) Smith, G. D.; Yoon, D. Y.; Zhu, W.; Ediger, M. D. *Macromolecules* **1994**, *27*, 5563.
- (26) Mansfield, M. *J. Chem. Phys.* **1980**, *72*, 3923.
- (27) Moe, N.; Ediger, M. D. *Polymer* **1996**, *37*, 1787.
- (28) Moe, N.; Ediger, M. D. *Macromolecules* **1995**, *28*, 2329.
- (29) (a) Maple, J. R.; Dinur, U.; Hagler, A. T. *Proc. Natl. Acad. Sci. U.S.A.* **1988**, *85*, 5350. (b) Maple, J. R.; Thacher, T. S.; Dinur, U.; Hagler, A. T. *Chem. Des. Automat. News* **1990**, *5* (9), 5.
- (30) Biosym Technologies Inc., San Diego, CA.
- (31) Another important feature of C–H vector correlation functions in the three environments is that they have qualitatively different shapes (see Figure 3). The long-time portion of the decay is nearly single exponential in solution and quite nonexponential in the melt. In this paper, we have not considered the relationship between the mechanism of local polymer dynamics and the C–H vector correlation function shapes.
- (32) Takeuchi, H.; Roe, R. *J. Chem. Phys.* **1991**, *94*, 7446.
- (33) Simulations by Smith *et al.* (Smith, G. D.; Yoon, D. Y.; Jaffe, R. L. *Macromolecules* **1995**, *28*, 5897) on *n*-C₄₄H₉₀ melts also show quite anisotropic dynamics, although not to the same degree as found by Takeuchi and Roe. Simulations of *cis*- and *trans*-polybutadiene melts by Kim and Mattice (Kim, E.-G.; Mattice, W. L. *J. Chem. Phys.* **1994**, *101*, 6242) show that the backbone geometry can play a large role: The *cis* chains were found to have relatively little relaxation anisotropy, similar to our *cis*-polyisoprene, while the local dynamics of the *trans*- chains were much more anisotropic.
- (34) These times are calculated from the trajectory length τ_{traj} , the total number of conformational transitions of a given type N_{trans} , and the number of torsions of that type N_{tors} such that $\tau = \tau_{\text{traj}} N_{\text{tors}} / N_{\text{trans}}$. The average transition time is calculated using the same equation except that all types of torsions are considered.
- (35) This was done by subtracting the infinite time values and normalizing the resulting functions (not shown).
- (36) For the purpose of this calculation, a repeat unit was defined to be the region between double bonds.
- (37) There were about 10 times more barrier crossings than conformational transitions in the melt and solution, and about 5 times more in vacuum.

MA960204T